



# Preclinical evaluation of a novel anterior non-fusion fixation device for atlantoaxial instability: an in vivo comparison study in a canine model

Xuan Cai<sup>1</sup> · Xiaoqing Yi<sup>2</sup> · Haopeng Li<sup>1</sup> · Xijing He<sup>1</sup>

Received: 24 June 2018 / Revised: 28 December 2018 / Accepted: 9 February 2019 / Published online: 13 February 2019  
© Springer-Verlag GmbH Germany, part of Springer Nature 2019

## Abstract

**Purpose** The Anterior Atlantoaxial Non-Fusion Fixation System (AANFS) was a novel motion preservation device for atlantoaxial instability to replace traditional fusion techniques. The purpose of this in vivo study was to evaluate the clinical features and biomechanical properties of this new device in a canine model by comparing it with a conventional method.

**Methods** Eighteen adult male canines were randomly divided into group 1, which received the AANFS replacement, group 2 which received the Harms rigid fixation procedures, and group 3, which served as the control group. Routine follow-up evaluations were performed postoperatively. Specimens were harvested 12 weeks after the operation. Biomechanical tests were conducted to obtain the range of motion (ROM) and neutral zone (NZ) at C1–C2 segment in different groups.

**Results** The canines successfully tolerated the entire experimental procedure. No significant differences were found in surgery time, blood loss and recovery time between the AANFS group and the Harms rigid fixation group. Radiological examinations revealed that the position of the implant was good. Biomechanical results showed that, compared with the intact group, the mean ROM and NZ in flexion, extension, lateral bending and rotation were significantly reduced after rigid fixation. However, after the AANFS implantation, ROM and NZ in all directions were similar to those of the intact state.

**Conclusions** This study for the first time provides an animal model for studying non-fusion strategies of upper cervical spine. The AANFS was able to maintain movement function of the atlantoaxial joint and may be an alternative to traditional fusion techniques.

## Graphical abstract

These slides can be retrieved under Electronic Supplementary Material.

The graphical abstract consists of three slides from a presentation. The first slide, titled 'Key points', lists five items: 1. in vivo, 2. canine model, 3. The Anterior Atlantoaxial Non-Fusion Fixation System (AANFS), 4. atlantoaxial instability, and 5. biomechanics. The second slide, titled 'Process for establishing the in vivo model', shows a series of seven photographs (A-G) illustrating the surgical steps: (A) Adequate exposure of the anterior surface of C1-C2, (B) the anterior arch of C1 was ground with a spherical drill bit, (C) exposure of the odontoid process, (D) after the odontoid resection, (E) after the AANFS was implanted, (F) after the Harms rigid fixation. The third slide, titled 'Take Home Messages', contains two points: 1. This study for the first time provides a convenient animal model for studying non-fusion strategies of upper cervical spine in vivo. 2. The Anterior Atlantoaxial Non-Fusion Fixation System (AANFS) was able to maintain atlantoaxial stability and movement function, and may be an alternative to traditional fusion techniques. Each slide includes the Spine Journal logo and the Springer logo.

**Keywords** In vivo · Canine model · Atlantoaxial instability · Non-fusion · Biomechanics

**Electronic supplementary material** The online version of this article (<https://doi.org/10.1007/s00586-019-05916-3>) contains supplementary material, which is available to authorized users.

Extended author information available on the last page of the article

## Introduction

Clinical studies have shown that decompression procedures such as odontoidectomy compromise the integrity and aggravate instability of atlantoaxial complex [1, 2]. Therefore, anterior or posterior atlantoaxial fusion should be performed to eliminate this instability [3–5]. Such decompression and fusion procedures are considered standard treatment for atlantoaxial instability diseases caused by congenital, traumatic, inflammatory, or neoplastic involvement [6, 7]. However, the long-term follow-up revealed that fusion of C1 to C2 will, of necessity, restrict head motion by about 50%. In a normal patient, this leaves a residual motion of  $\pm 45^\circ$  [8]. Loss of rotation function will have a long-term negative impact on the physiological and biomechanical functions of the cervical spine and may adversely impact patient quality of life.

In recent years, developments in the non-fusion technology have introduced a new era of managing pathology conditions through motion preservation and retention of spinal flexibility. Although it has some obvious potential benefits, previous attempts to develop non-fusion devices for upper cervical spine have been met with limited success. To resolve this problem, we designed a motion preservation device, the Anterior Atlantoaxial Non-Fusion Fixation System (AANFS), to preserve partial or complete movement of the atlantoaxial to replace traditional fusion techniques. The biomechanical tests in human cadaveric specimens revealed that the AANFS maintains atlantoaxial stability and partial movement function, demonstrating certain value for its clinical applications [9, 10]. However, in vitro experiments only provide short-term, perioperative biomechanical results. It is premature to state that the AANFS will be as effective in its function as an artificial knee or hip joint. The long-term safety, feasibility,

effectiveness and biological degradation of the AANFS prosthesis remain unknown.

In our previous study (unpublished), we found that canines had similar atlanto-odontoid joints to humans; thus, they may provide a convenient animal model for in vivo experiments of the upper cervical spine. In the present study, we designed an atlantoaxial non-fusion model in canines for the first time and performed in vivo and in vitro experiments to compare the clinical features and biomechanical properties of the AANFS with those of the intact state and the anterior plate fusion state.

## Methods

### AANFS implants

The AANFS is composed of a titanium alloy and includes the C1 component, C2 component, joint component and screws (Fig. 1). The C1 component consists of a symmetrical arc-shaped fixing plate and rotating cuff. The C2 component is composed of a fixing plate and base, with a hemispherical joint socket above the base. The joint component is composed of a cylindrical rotating axle and spherical joint head. The rotating axle forms a pivot joint with the rotating cuff of the C1 component; the spherical joint head forms a ball-and-socket joint with the C2 component. The pivot joint coordinates with the ball-and-socket joint to allow multiaxial movement of the C1–C2 segment. C1 components are fixated using lateral mass screws, whereas C2 components are fixated using anterior articular mass screws.

### Experimental animals

Eighteen healthy male adult mixed-breed (same origin) canines, weighing  $20 \pm 1.0$  kg and aged  $2 \pm 0.2$  years, were

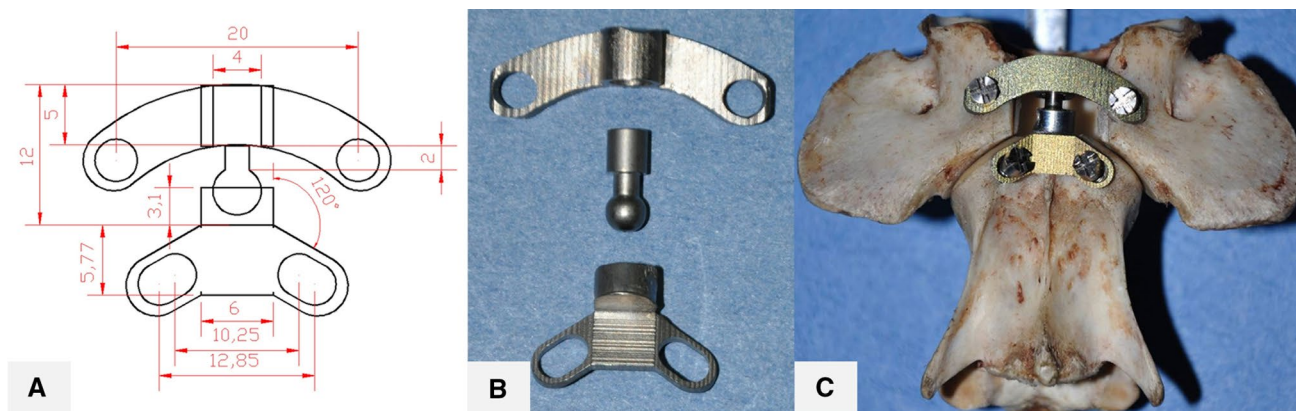


**Fig. 1** Schematic diagram and photographs of the Anterior Atlantoaxial Non-Fusion Fixation System (AANFS). **a** Schematic diagram of the AANFS; **b** actual photo of the AANFS; **c** schematic illustration of the AANFS on the specimen

used in this study. The canines were randomly divided into three groups: six in the prosthesis implantation group receiving AANFS implantation (group 1), six in the fusion group undergoing Harms plate rigid fixation (group 2), and six in the control group undergoing sham surgery (group 3).

### Surgical procedure

The canines were fasted 24 h and were intramuscularly injected with cefazolin sodium (20 mg, IM) 30 min before surgery. Under general anesthesia (10 mg ketamine and 30 mg/kg of 3% pentobarbital sodium), the dogs were placed in supine position, and a 6-cm anterior-medial incision was made in the neck. The cervical spine was accessed via the space between the vascular sheath and visceral sheath. The bilateral longus colli muscles were dissected to expose the anterior surface of C1–C2, which was confirmed by C-arm radiography.

For the AANFS implantation procedure (group 1), a high-speed grinding drill was used to carefully remove the C1 anterior arch and odontoid process. The apical,

alar, and transverse ligament attachments to the odontoid process were carefully resected to decompress and visualize the duration (Fig. 2a–d). The assembled AANFS was placed in the center of the decompression site. After determining the C1 component screw entry points, the lateral mass screws were directly inserted. The C2 component fixation screws (anterior articular mass screws) were inserted via the adjustable oval screw holes based on the individual anatomy of the canine axis. Figure 2e shows the AANFS in place after being implanted over a decompressed specimen.

For the Harms plate fixation (group 2), the Harms plate was placed in the center of the decompression site after resecting the ventral arch of C1 and odontoid. The lateral mass screws and vertebral screws were inserted separately. The bone graft was then placed between the lateral mass facets of the atlantoaxial joint (Fig. 2f). The control group underwent sham surgery to expose the anterior surface of C1–C2. For each experimental canine, sterile saline was used to rinse the surgical wound, and the wounds were closed in layers to complete the procedure.

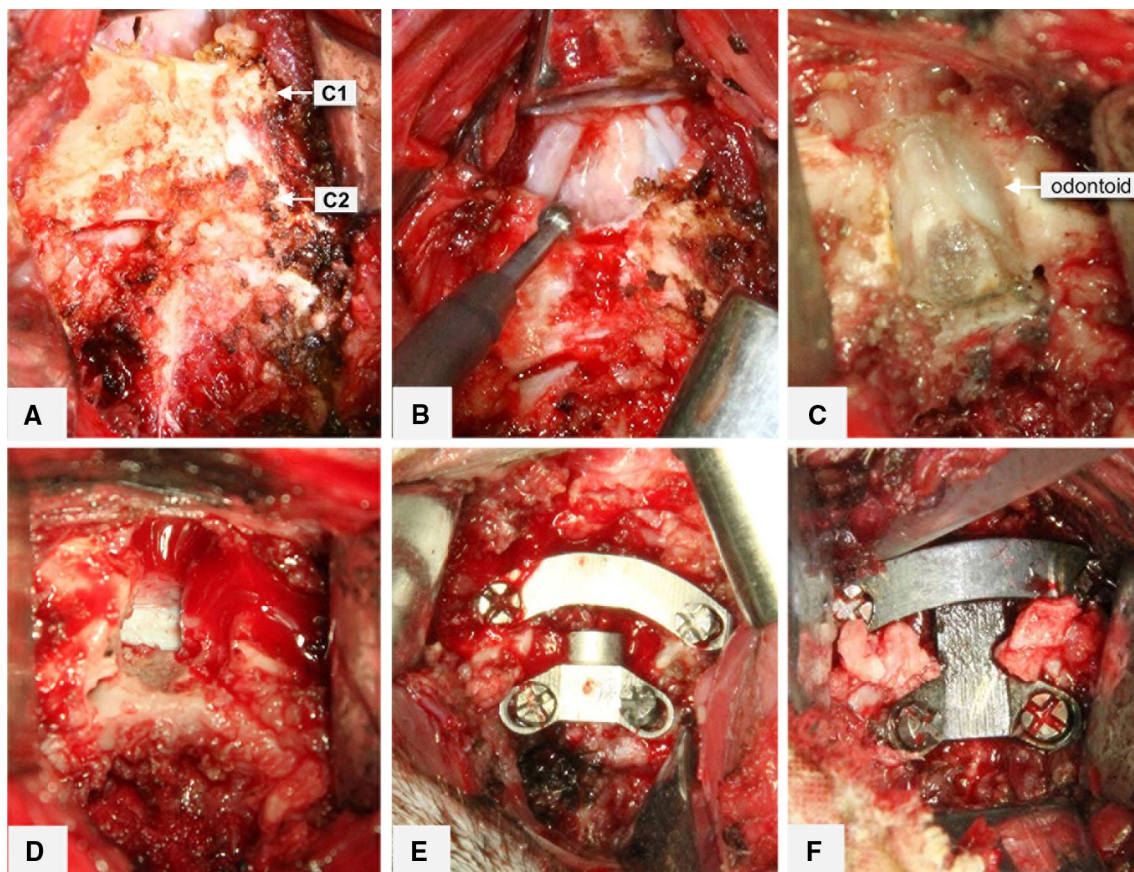


**Fig. 2** Process for establishing the in vivo model. **a** Adequate exposure of the anterior surface of C1–C2; **b** the anterior arch of C1 was ground with a spherical drill bit; **c** exposure of the odontoid process.

**d** After the odontoid resection; **e** after the AANFS was implanted; **f** after the Harms rigid fixation

## Postoperative management

For each experimental canine, operation time, intraoperative blood loss, and the starting times for postoperative eating and walking were documented in detail. The necks of the canines in the AANFS implantation group and the fusion group were immobilized by a neck cast for 1 month. Cefazolin sodium (20 mg, IM, qd) injection continued for 3 days after surgery. Surgical wounds were examined regularly. Radiography and CT scans were taken preoperatively 1 and 12 weeks after surgery. The positions of the AANFS were evaluated in detail using 3D reconstruction modeling. All experimental canines were housed in the animal center and euthanized with an overdose of pentobarbital 12 weeks after the operation. Complete postmortem examinations were performed on all animals. Specimens of the liver, spleen, mesenteric lymph nodes, and soft tissues adjacent to implants were collected, fixed in neutral buffered formalin, and submitted for histology to assess the safety of the prosthesis. A segment from the base of the occipital bone to the lower portion of the C3 was harvested. The collected specimens were stored in a double-layer sealed plastic bag in a  $-80^{\circ}\text{C}$  freezer for later use.

## Biomechanical testing

Before the biomechanical tests, the specimens were removed from the  $-80^{\circ}\text{C}$  freezer. After thawing at room temperature, the skin and muscle tissues of the specimens were removed, and the osteoligamentous structures, such as the ligaments and facet joint capsule, were integrally preserved. All specimens were divided into the following four groups: (1) the AANFS implantation group, (2) the Harms rigid fixation group, (3) the control group (intact group), and (4) after odontoidectomy of the intact group (decompression group).

The specimens were embedded in quick-drying epoxy resin in a specialized metal mold. The bottom of the C3 vertebral body was positioned horizontally to ensure that

the atlanto-occipital and atlantoaxial joints were naturally positioned. The biomechanical specimens were placed in a multi-channel spine testing device (MTS 858 Bionix machine, MTS System Inc., Minneapolis, MN, USA). Two markers were rigidly attached to the C1 and C2 vertebrae. Each marker included four unaligned infrared light-emitting diodes. Three-dimensional flexibility tests were conducted per the protocol established in our previous studies [9, 10]. Specimens were subjected to continuous torque loading up to 1.0 Nm at a rate of  $0.5^{\circ}/\text{second}$  by a multi-channel spine testing device to induce six-directional movements (as shown in Fig. 3). A three-dimensional optoelectronic camera system (Optotrak 3020; Northern Digital, Waterloo, Canada) was used to acquire each marker's spatial position at a rate of 100 Hz during the loading phase. Range of motion (ROM) and neutral zone (NZ) were used to describe the segmental motion of each specimen.

## Histological evaluation

After biomechanical testing, the cervical spine specimens were fixed in 4% paraformaldehyde and 5% glutaraldehyde for 2 weeks. Specimens were dehydrated in gradient ethanol and embedded in polymethylmethacrylate. Transverse sections ( $100\ \mu\text{m}$  thick) were cut on a Leica SP1600 sawing microtome (Leica, Nussloch, Germany). After grinding the sections to the appropriate thickness, modified paucan trichrome staining was used for transmitted light microscopy. Sections were examined for the presence or absence of inflammatory cellular infiltrates, particulate debris, and evidence of implant loosening.

## Statistical analysis

All results were analyzed using SPSS version 19.0 (Chicago, IL, USA). Statistical analysis was performed using one-way analysis of variance, and Fisher's least-squares difference

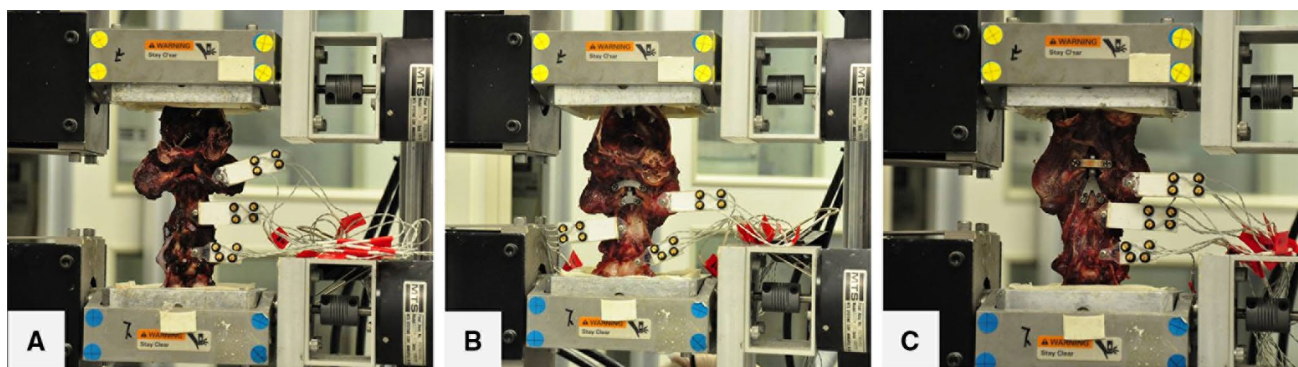


**Fig. 3** Biomechanical models. **a** Decompression group; **b** the AANFS implantation group; **c** fixation group

was used for post hoc analysis. *P* values less than 0.05 were considered statistically significant.

## Results

All surgeries were successful, and all canines recovered well. The incisions in all experimental canines healed well, with no infections. For each experimental canine, the operative time, intraoperative blood loss, and starting time for postoperative eating and walking are presented in Table 1. No significant differences were found between the AANFS implantation group and the Harms rigid fixation group. Postoperative radiography images revealed satisfactory positions of the implants, and no joint dislocation, bone fracture, loosened/fractured screws, or screws penetrating the spinal canal were observed in the AANFS implantation group or the Harms rigid fixation group (Fig. 4). CT scan and three-dimensional reconstruction imaging revealed that the atlanto-odontoid joint was reconstructed by the AANFS and that the screws were located in a pre-designed trajectory (Fig. 5). No evidence of spinal cord compression was noted. After sacrificed, gross examinations were performed on all animals. In the AANFS implantation group, the fixing plate of C1 and

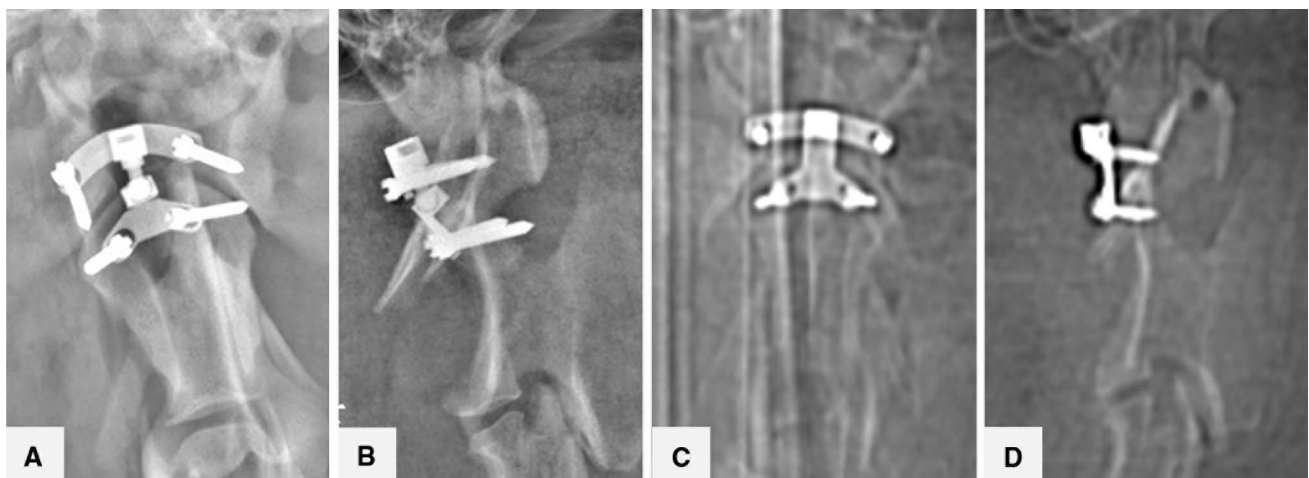
C2 components was typically surrounded by loose fibrous tissue that was easily removed. The joint component was firmly attached to the odontoid base of the C2 vertebral body. No fibrous tissue and visible debris were observed in the joint space of the prosthesis, and there was no evidence of screw loosening was found. HE staining showed that the soft tissue around the prosthesis, draining lymph nodes, liver, and spleen were normal. No hemosiderin deposition, inflammatory response, and metal particles were observed.

Table 2 presents the relative ROM and NZ of the C1–C2 segment in flexion, extension, lateral bending, and axial rotation among the groups. The primary motion pattern of the intact C1–C2 segment was rotation accompanied by partial lateral bending and flexion and extension. Compared with the intact group, ROM and NZ of the C1–C2 segment with anterior arch and odontoid process excision (decompression group) were significantly increased ( $P < 0.05$ ) in the flexion, extension, lateral bending, and rotation. However, after the AANFS replacement, ROM and NZ of the C1–C2 segment in flexion, extension, lateral bending, and rotation were similar to those of the intact state ( $P > 0.05$ ). In addition, the mean ROM and NZ in flexion, extension, lateral bending, and rotation were significantly reduced after Harms plate fixation ( $P < 0.05$ ) compared with those in the intact state, decompression, or AANFS implantation groups.

**Table 1** Surgery characteristics of the three different groups

	Surgery time (min)	Blood loss (ml)	Recovery time (h)	Eating time (h)
Sham control	15 ± 4	4 ± 2	1.5 ± 0.5	2.0 ± 0.2
AANFS implantation	80 ± 12	26 ± 4	3.2 ± 0.8	5.4 ± 1.4
Rigid fixation	72 ± 10	24 ± 6	4.1 ± 1.2	5.8 ± 2.0

No significant differences were found between the AANFS implantation group and the Harms rigid fixation group



**Fig. 4** X-ray images of canines in the AANFS implantation group and Harms rigid fixation group 12 weeks after the surgery. **a** Anteroposterior view of the AANFS implantation; **b** lateral view; **c** anteroposterior view of the Harms rigid fixation. **d** Lateral view

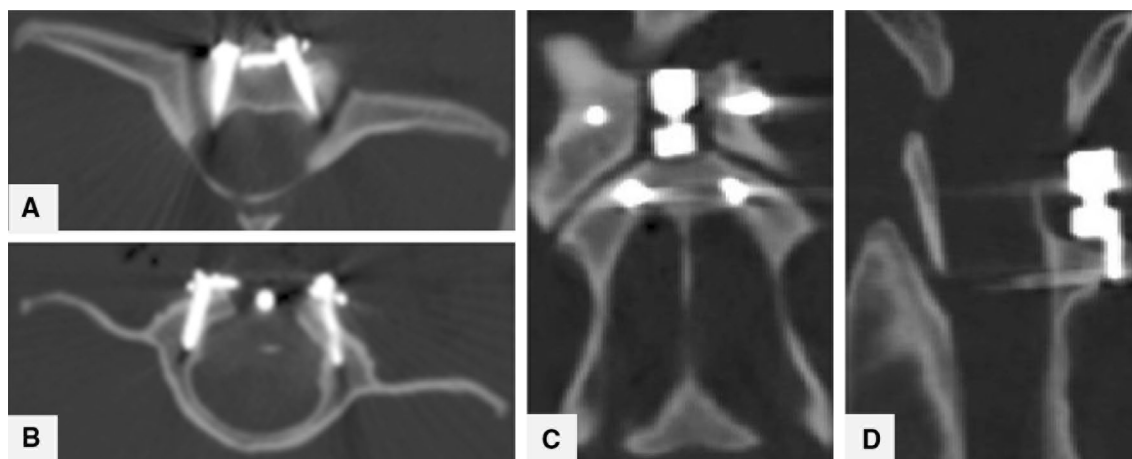


**Fig. 5** CT images of canines in the AANFS implantation group 12 weeks after the surgery. **a** Transverse view of anterior C2 articular mass screws; **b** transverse views of C1 lateral mass screws; **c** 3D

reconstruction of coronal view of the AANFS; **d** 3D reconstruction of sagittal view of the AANFS

**Table 2** ROM and NZ of the specimens of the four groups in all directions (in degrees)

Motion	Control	Unstable	AANFS	Harms
<b>ROM</b>				
Flexion	6.24 ± 0.75	9.36 ± 1.18*	5.89 ± 1.56 <sup>†‡</sup>	2.54 ± 0.91* <sup>†</sup>
Extension	8.89 ± 0.83	10.87 ± 0.98*	7.88 ± 1.88 <sup>†‡</sup>	3.04 ± 0.35* <sup>†</sup>
Lateral bending	4.51 ± 0.66	8.53 ± 1.32*	4.02 ± 1.35 <sup>†‡</sup>	1.19 ± 0.42* <sup>†</sup>
Axial rotation	14.94 ± 2.68	20.42 ± 2.32*	16.27 ± 2.14 <sup>†‡</sup>	8.34 ± 1.45* <sup>†</sup>
<b>NZ</b>				
Flexion	2.25 ± 0.86	4.36 ± 0.18*	2.09 ± 0.56 <sup>†‡</sup>	1.14 ± 0.16* <sup>†</sup>
Extension	2.97 ± 0.54	4.87 ± 1.98*	2.68 ± 0.48 <sup>†‡</sup>	1.83 ± 0.15* <sup>†</sup>
Lateral bending	1.01 ± 0.07	2.53 ± 0.82*	0.92 ± 0.35 <sup>†‡</sup>	0.56 ± 0.07* <sup>†</sup>
Axial rotation	5.58 ± 1.39	9.42 ± 2.32*	6.27 ± 2.14 <sup>†‡</sup>	3.93 ± 0.17* <sup>†</sup>

Values for axial rotation and lateral bending summate both right and left sides

ROM range of motion, NZ neutral zone, AANFS Anterior Atlantoaxial Non-Fusion Fixation System

\*Indicates statistical difference from intact condition ( $P < .05$ )

<sup>†</sup>Indicates statistical difference from unstable condition ( $P < .05$ )

<sup>‡</sup>Indicates statistical difference from Harms rigid fixation ( $P < .05$ )

Histological sections of the canine cervical spines 12 weeks after surgery showed newly formed bone around the fixation screws (Fig. 6). No inflammatory response or significant metallic wear debris at the implant–bone interface was found, indicating favorable biocompatibility of the prosthesis.

## Discussion

Atlantoaxial instability can result from disruption of the bony or ligamentous elements or both. The unique anatomical and biomechanical aspects of the atlantoaxial complex present specific challenges for operative stabilization of this region. The surgical management of atlantoaxial instability

has evolved due to advances in spinal biomechanics and instrumentation systems. Rigid C1–2 fixation using screws or screw/rod constructs is increasingly being advocated since it is associated with high fusion rates and provides immediate spinal stability in all planes [11]. However, the long-term follow-up revealed that fusion of C1 to C2 will, of necessity, restrict head motion by about 50%. In a normal patient, this leaves a residual motion of  $\pm 45^\circ$ . Loss of rotation function will have a long-term negative impact on the physiological and biomechanical functions of the cervical spine and may adversely impact patient quality of life [12]. Thus, it is necessary to explore how to maximally preserve the physiological motion of the C1–C2 segment while firmly fixing it. Recent developments in the non-fusion technology have introduced a new era of managing pathology conditions

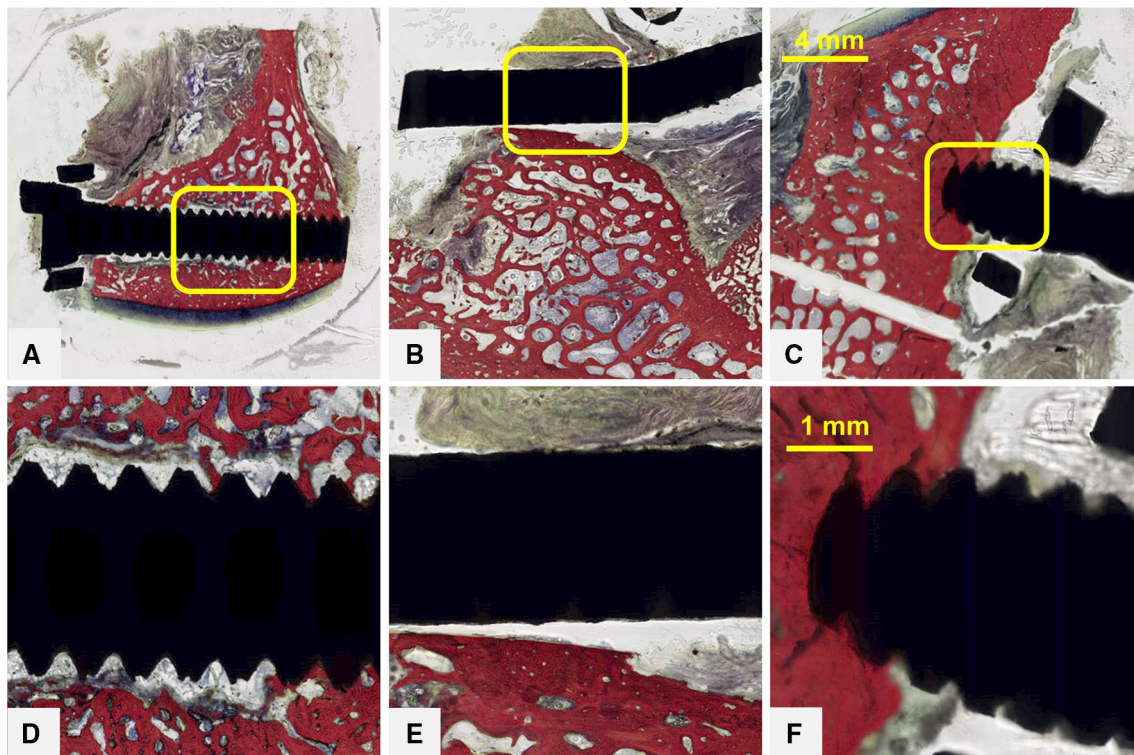


**Fig. 6** Histological images of the specimens in the AANFS implantation group 12 weeks after the surgery. **a, d** 10X- and 40X-magnified images at the level of C1 lateral mass screws; **b, e** 10X- and

40X-magnified images at the level of fixing plate of C2 component; **c, f** 10X- and 40X-magnified images at the level of anterior C2 articular mass screws

through motion preservation and retention of spinal flexibility. This widely expanded armamentarium available to the spine specialist has allowed surgeons to address cases with evermore challenging biomechanical presentations. To date, non-fusion techniques used in clinical practice include artificial disks, artificial nucleus pulposus, and posterior dynamic spine stabilization systems (such as spinous process spacers and facet joint replacement) [13]. However, current research on dynamically stabilizing the atlantoaxial joint remains limited. Goel et al. [14] reported an artificial atlantoaxial lateral mass joint prosthesis and proposed the mechanism of its insertion and function. However, the complexity of the surgery made use of it a less attractive option.

Given that the most important function of the C1–C2 segment is rotational head movement, our research team designed the AANFS to stabilize and preserve movement of the C1–C2 segment. Theoretically, intact anterior C1–C2 structures, including C1 lateral mass and C2 vertebrae, were the minimum anatomical requirements for the implant of the AANFS. Biomechanical testing in cadavers revealed that this prosthesis achieves sufficient decompression and preserves stability and motion [10]. Nonetheless, it is important to realize that even the most sophisticated biomechanical testing setup is not capable of evaluating the biologic responses of an organism to a surgical intervention and a

foreign body implantation. Certain reconstructions that appear biomechanically superior in a laboratory may not be clinically appropriate secondary to bulky design, low available volume for bony ingrowth, technically challenging surgical technique, or other factors. In addition, *in vitro* experiments cannot completely simulate the physiological function *in vivo*. The long-term safety, efficacy, and biological degradation of the AANFS remain unknown. Therefore, the AANFS must be further evaluated using *in vivo* animal models in preclinical testing.

Animal models for studying spinal non-fusion techniques have been reported in the literature on animals including canines, goats, and nonhuman primates (e.g., chimpanzees and baboons). Of these models, canines are a good model often used to evaluate implants in cervical spine research [15–17]. Biomechanical studies found that the canine spine was mainly loaded along its long axis, similar to human spines [18]. Moreover, canines are of medium size with typical atlanto-odontoid joints, which have similar ranges of movement to the upper cervical spine in humans. Therefore, we believe canines provide a suitable animal model for evaluating the AANFS *in vivo*, given a lack of primates. Consequently, we designed an AANFS device for canines based on anatomical parameters and performed this *in vivo* study. In this study, no incision or deep tissue infections

were reported. During the entire operation, canine vital signs remained stable, and the operative time and intraoperative blood loss were similar to those in the Harms plate fusion procedure. The animals could walk near normally and eat without difficulty 3 and 5 h, respectively, after surgery. Radiography and CT scans revealed that the AANFS positions were satisfactory and that the screws were located in a pre-designed trajectory. No neurological complications were found. Although the AANFS dislocation (the most significant postoperative complication) was anticipated as a possible concern in this animal model, no dislocations were observed during the experimental period. In non-fusion spinal implants, poor wear resistance of titanium alloys has raised the concern of an inflammatory reaction loosening the implants due to osteolysis. In the present study, no inflammatory response or metallic wear debris was found at the implant–bone interface, the soft tissue around the prosthesis, draining lymph nodes, liver, and spleen in the 12-week in vivo animal model, indicating favorable prosthesis biocompatibility.

Johnson et al. [18] systematically evaluated the biomechanics of the whole canine spine broken down into individual motion segments. They then compared their data with human ROM values published by White and Panjabi. The authors reported similarities in ROM, NZ, and stiffness between the two models under axial rotation. The lateral bending and flexion–extension range was somewhat lower, however, still within the acceptable range. In this study, we found that, in the intact state, the primary motion pattern of the C1–C2 segment is axial rotation. The instantaneous rotation axes are located in the atlanto-odontoid joint. After excising the anterior arch and odontoid process, the instantaneous rotation axes will move posteriorly to the bilateral facets [2, 19]. Segment stability is significantly reduced due to loss of atlanto-odontoid joints. This study demonstrated that ROM and NZ in the C1–C2 segments increased significantly after odontoidectomy in terms of flexion, extension, lateral bending, and rotation compared with the intact state. In general, flexion, extension, and lateral bending of the normal C1–C2 segment are limited. However, completely limited lateral bending, flexion, or extension may increase fixation screw stress, possibly loosening the prosthesis. Therefore, the ball-and-socket structure of the AANFS was designed to ensure a 60° range of motion in flexion, extension, and lateral bending. In addition, the pivot joint design guarantees unrestricted rotation of the C1–C2 segment as well as coupled motions. Theoretically, the close coordination between the ball-and-socket and pivot joints can rebuild the atlantoaxial buckling, which causes the instantaneous rotation axes to reposition in the atlanto-odontoid joint. This study demonstrated that after AANFS implantation, ROM and NZ of the atlantoaxial joint in flexion, extension, lateral bending, and rotation were similar to those in the intact

group. Compared with the intact state, decompression, and AANFS implantation state, ROM and NZ of the C1–C2 segment in all directions significantly decreased after Harms plate fixation. This result is consistent with that from the biomechanical study of Harms plate fusion in humans [20]. The above results indicate that the AANFS successfully restored motion, which was generally closer to the intact condition.

Several limitations are inherent to this study. First, the follow-up duration was limited; thus, a longer study period should be investigated before long-term conclusions are reached on the durability and stability of the AANFS. The long-term stability of the AANFS in vivo depends on the osteointegration of bone–implant interface, which can be affected by many factors, such as prosthesis design, surface texture, biocompatibility, bioactive coating, and the biomechanical properties of the surrounding bone. Several strategies have been developed to enhance the bone–implant interface in mechanically demanding situations, including the use of hydroxyapatite (HA) coating. Experimental and clinical studies have shown that both osteointegration and strength at the interface between bone and HA-coated implants are substantially better than those between bone and uncoated implants [21]. Therefore, we are planning to conduct further experiment aiming at improving the durability and stabilization capacity of AANFS for clinical application, such as applying HA coating on the surface of AANFS to improve the bone–implant integration for long-term stability. Second, these findings are of limited significance because canines do not walk upright, and their anatomical structures and physiological features differ from those of humans. Thus, primates are ideal experimental animals for obtaining results that more closely mimic clinical reality, and data obtained from primates may be more valuable in practice.

## Conclusions

Canine was an excellent animal model for in vivo experiments of upper cervical spine. Biomechanical results showed that AANFS implantation preserved the ROM and NZ of the C1–C2 segment and, thus, may be an alternative to the anterior fusion method.

**Acknowledgements** This study was sponsored by National Natural Science Youth Funds of China (Program No.: 81601955) (<http://www.nsf.gov.cn>). The funders had no role in study design, data collection and analysis, decision to publish, or preparation of the manuscript.

## Compliance with ethical standards

**Conflict of interest** The authors declare that they have no competing interests.

**Ethics statement** This study was carried out in strict accordance with the recommendations in the Guide for the Care and Use of Laboratory Animals of the National Institutes of Health. The protocol was approved by the Committee of the Second Affiliated Hospital of Xi'an Jiaotong University (Permit Number: 2016-20). All surgery was performed under sodium pentobarbital anesthesia, and all efforts were made to minimize suffering.

**Data availability** All data generated or analyzed during this study are included in this article.

## References

- Nakagawa H, Yagi K (2014) Advancement in atlantoaxial fixation. *World Neurosurg* 82:e143–e144
- Dickman CA, Crawford NR, Brantley AG, Sonntag VK (1995) Biomechanical effects of transoral odontoidectomy. *Neurosurgery* 36:1146–1152
- Elliott RE, Tanweer O, Boah A, Morsi A, Ma T, Frempong-Boadu A et al (2014) Outcome comparison of atlantoaxial fusion with transarticular screws and screw-rod constructs: meta-analysis and review of literature. *J Spinal Disord Tech* 27:11–28
- Du JY, Aichmair A, Kueper J, Wright T, Lebl DR (2015) Biomechanical analysis of screw constructs for atlantoaxial fixation in cadavers: a systematic review and meta-analysis. *J Neurosurg Spine* 22:151–161
- Rajinda P, Towiwat S, Chirappapha P (2017) Comparison of outcomes after atlantoaxial fusion with C1 lateral mass-C2 pedicle screws and C1–C2 transarticular screws. *Eur Spine J* 26:1064–1072
- Elbadrawi AM, Elkhateeb TM (2017) Transoral approach for odontoidectomy efficacy and safety. *HSS J* 13:276–281
- Shriver MF, Kshetry VR, Sindwani R, Woodard T, Benzel EC, Recinos PF (2016) Transoral and transnasal odontoidectomy complications: a systematic review and meta-analysis. *Clin Neurol Neurosurg* 148:121–129
- Derman PB, Lampe LP, Lyman S, Kueper J, Pan TJ, Girardi FP et al (2016) Atlantoaxial fusion: sixteen years of epidemiology, indications, and complications in New York State. *Spine (Phila Pa 1976)* 41:1586–1592
- Cai X, He X, Li H, Wang D (2013) Total atlanto-odontoid joint arthroplasty system: a novel motion preservation device for atlantoaxial instability after odontoidectomy. *Spine (Phila Pa 1976)* 38:451–457
- Lu B, He X, Zhao CG, Li HP, Wang D (2009) Biomechanical study of artificial atlanto-odontoid joint. *Spine (Phila Pa 1976)* 34:1893–1899
- Goel A, Desai KI, Muzumdar DP (2002) Atlantoaxial fixation using plate and screw method: a report of 160 treated patients. *Neurosurgery* 51:1351–1356
- Tanenbaum JE, Lubelski D, Rosenbaum BP, Thompson NR, Benzel EC, Mroz TE (2016) Predictors of outcomes and hospital charges following atlantoaxial fusion. *Spine J* 16:608–618
- Skeppholm M, Lindgren L, Henriques T, Vavruch L, Löfgren H, Olerud C (2015) The Discover artificial disc replacement versus fusion in cervical radiculopathy—a randomized controlled outcome trial with 2-year follow-up. *Spine J* 15:1284–1294
- Goel A (2015) Artificial atlantoaxial joint: is it a possible option? *J Craniovertebr Junction Spine* 6:147–148
- Moriguchi Y, Mojica-Santiago J, Grunert P, Pennicooke B, Berlin C, Khair T et al (2017) Total disc replacement using tissue-engineered intervertebral discs in the canine cervical spine. *PLoS ONE* 12:e0185716
- Grunert P, Moriguchi Y, Grossbard BP, Ricart Arbona RJ, Bonassar LJ, Härtl R (2017) Degenerative changes of the canine cervical spine after discectomy procedures, an in vivo study. *BMC Vet Res* 13:193
- Farrokhi MR, Torabinezhad S, Ghajar KA (2010) Pilot study of a new acrylic cage in a dog cervical spine fusion model. *J Spinal Disord Tech* 23:272–277
- Johnson JA, da Costa RC, Bhattacharya S, Goel V, Allen MJ (2011) Kinematic motion patterns of the cranial and caudal canine cervical spine. *Vet Surg* 40:720–727
- Shriver MF, Kshetry VR, Sindwani R, Woodard T, Benzel EC, Recinos PF (2016) Transoral and transnasal odontoidectomy complications: a systematic review and meta-analysis. *Clin Neurol Neurosurg* 148:121–129
- Kim SM, Lim TJ, Paterno J, Hwang TJ, Lee KW, Balabhadra RS et al (2004) Biomechanical comparison of anterior and posterior stabilization methods in atlantoaxial instability. *J Neurosurg* 100(3 Suppl Spine):277–283
- Ohe M, Moridaira H, Inami S, Takeuchi D, Nohara Y, Taneichi H (2018) Pedicle screws with a thin hydroxyapatite coating for improving fixation at the bone-implant interface in the osteoporotic spine: experimental study in a porcine model. *J Neurosurg Spine* 28:679–687

**Publisher's Note** Springer Nature remains neutral with regard to jurisdictional claims in published maps and institutional affiliations.

## Affiliations

Xuan Cai<sup>1</sup> · Xiaoqing Yi<sup>2</sup> · Haopeng Li<sup>1</sup> · Xijing He<sup>1</sup> 

✉ Xijing He  
xijinghe@yahoo.com

<sup>1</sup> Department of Orthopaedic Surgery, Second Affiliated Hospital of Xi'an Jiaotong University, Xi'an, Shaanxi, People's Republic of China

<sup>2</sup> Department of Pediatrics, Second Affiliated Hospital of Xi'an Jiaotong University, Xi'an, Shaanxi, People's Republic of China